Adsorption and Diffusion of Supercritical Carbon Dioxide in Slit Pores

ARTICLE *in* LANGMUIR · OCTOBER 2000

Impact Factor: 4.46 · DOI: 10.1021/la000216e

2 AUTHORS, INCLUDING:

Jian Zhou
South China University of Technology
84 PUBLICATIONS **1,597** CITATIONS

Adsorption and Diffusion of Supercritical Carbon Dioxide in Slit Pores

Jian Zhou and Wenchuan Wang*

College of Chemical Engineering, Beijing University of Chemical Technology, Beijing 100029, China

Received February 14, 2000. In Final Form: June 27, 2000

A combination of grand canonical Monte Carlo and molecular dynamics methods has been used to investigate the adsorption and diffusion of carbon dioxide confined in seven slit carbon pores from 0.744 to 3.72 nm from subcritical to supercritical conditions. Adsorption isotherms and microstructures of carbon dioxide molecules in slit carbon pores are analyzed. The effects of pore size and operating conditions on the parallel and perpendicular diffusion coefficients are examined. The diffusion coefficients of CO_2 molecules confined in a slit pore in supercritical conditions strongly depend on the pore fluid density. The parallel diffusion coefficients are on the magnitude of $10^{-9} m^2 \cdot s^{-1}$, a typical liquidlike value. For the pores of reduced width larger than 4.0, the parallel diffusion coefficients are generally 10−20 times greater than the perpendicular ones. When the pressure is in the range 2−10 MPa, the parallel diffusion coefficients are in the range $(1.3-2.8) \times 10^{-9}$ $m^2 \cdot s^{-1}$ at 323 K, while they are $(2.0-5.3) \times 10^{-9}$ $m^2 \cdot s^{-1}$ at 348 K. Diffusion coefficients parallel and normal to the walls at supercritical temperatures are both 5−15 times larger than those at subcritical temperatures.

1. Introduction

Supercritical fluids (SCFs) exhibit liquidlike density and dissolution power, and gaslike viscosity and transport behavior. A common problem in the gas phase catalytic reaction is that catalyst pores can be clogged and hot spots can be developed if the waxes are not removed.[1] Therefore, the enhanced solvent properties and mass transfer characteristics of SCFs are extremely attractive for supercritical catalytic reaction processes.[1−3] CO_2 has been widely used as a solvent in supercritical reaction processes because of the advantages of mild critical condition (T_c = 304.2 K, P_c = 7.38 MPa), cheap, readily available, nonflammability, nontoxity, and environmentally benign.

Activated carbons, which are widely used in gas separation, purification, and catalytic reaction, have large internal specific surface area and almost uniform pore size of several molecular diameters. It has long been recognized that physical properties of a fluid confined in these porous materials differ significantly from those of the bulk fluid. Computer simulation[4,5] has been used to investigate surface-driven phase transitions,[6−9] methane storage,[10,11] and gas separation, [12] etc. However, relatively less attention has been paid to the adsorption at supercritical temperatures. Tan and Gubbins[13] investigated the adsorption behavior of methane and ethylene in slitlike carbon micropores at supercritical temperatures by using both computer simulation and a nonlocal density functional theory. In addition, Nitta et al.[14] simulated adsorption equilibrium characteristics in supercritical fluids.

An important phenomenon of a fluid confined in porous media is the hindered diffusion.[15] Quantitative prediction of the hindered diffusion is important in guiding experiments and improving engineering designs in diversified applications, such as molecular sieve operations, catalytic processing of heavy liquid petroleum fractions, gel permeation chromatography, and permeation through natural and synthetic membranes.[16] Magda et al.[17] first studied the self-diffusion in smooth-wall slit pores by molecular dynamics (MD) method. They correlated the diffusion coefficients with the average density of the pore fluid. Schoen et al.[18] calculated the self-diffusion coefficients of rare gases for a model slit pore of two parallel face-centered cubic (100) planes. Demi and Nicholson[19] reported the effect of the length of sphere to length of cylinder on the self-diffusion of Lennard-Jones (LJ) fluids confined in a

* Corresponding author. E-mail: wangwc@buct.edu.cn. Tel: +86-10−64433776. Fax: +86-10-64436781.

(1) Saito, S. *J. Supercrit. Fluids* **1995**, *8*, 177.
(2) Savage, P. E.; Gopalan, S.; Mizan, T. I.; Martino, C. J.; Brock, E. E. *AIChE J* **1995**, *41*, 1723.
(3) Savage, P. E. *Chem. Rev.* **1999**, *99*, 603.
(4) Allen, M. P.; Tildesley, D. J. *Computer Simulation of Liquids;* Clarendon Press: Oxford, UK, 1987.
(5) Frenkel, D.; Smit, B. *Understanding molecular simulation;* Academic Press: Amsterdam, 1996.
(6) Peterson, B. K.; Gubbins, K. E. *Mol. Phys.* **1987**, *62*, 215.
(7) Jiang, S.; Rhykerd, C. L.; Gubbins, K. E. *Mol. Phys.* **1993**, *79*, 373.
(8) Wu, G. W.; Chan, K. Y. *Fluid Phase Equilib.* **1997**, *132*, 21.
(9) Gubbins, K. E.; Sliwinska-Bartkowiak, M.; Suh, S. H. *Mol. Simul.* **1996**, *17*, 333.
(10) Matranga, K. R.; Myers, A. L.; Glandt, E. D. *Chem. Eng. Sci.* **1992**, *47*, 1569.
(11) Cao, D.; Gao, G.; Wang, W. *J. Chem. Ind. Eng. (China)* **2000**, *51*, 23.
(12) Nicholson, D.; Gubbins, K. E. *J. Chem. Phys.* **1996**, *104*, 8126.
(13) Tan, Z.; Gubbins, K. E. *J. Phys. Chem.* **1990**, *94*, 6061.
(14) Nitta, T.; Shigeta, T. *Fluid Phase Equilib.* **1998**, *144*, 245.
(15) Deen, W. M. *AIChE J.* **1987**, *33*, 1409.
(16) Satterfield, C. N.; Colton C. K.; Pitcher W. H. *AIChE J.* **1973**, *19*, 628.
(17) Magda, J. J.; Tirrell, M.; Davis, H. T. *J. Chem. Phys.* **1985**, *83*, 1888.
(18) Schoen, M.; Cushman, J. H.; Diestler, D. J.; Rhykerd, C. L. *J. Chem. Phys.* **1988**, *88*, 1394.
(19) Demi, T.; Nicholson D. *J. Chem. Soc., Faraday Trans.* **1991**, *87*, 3791.

10.1021/la000216e CCC: $19.00
Published on Web 09/15/2000

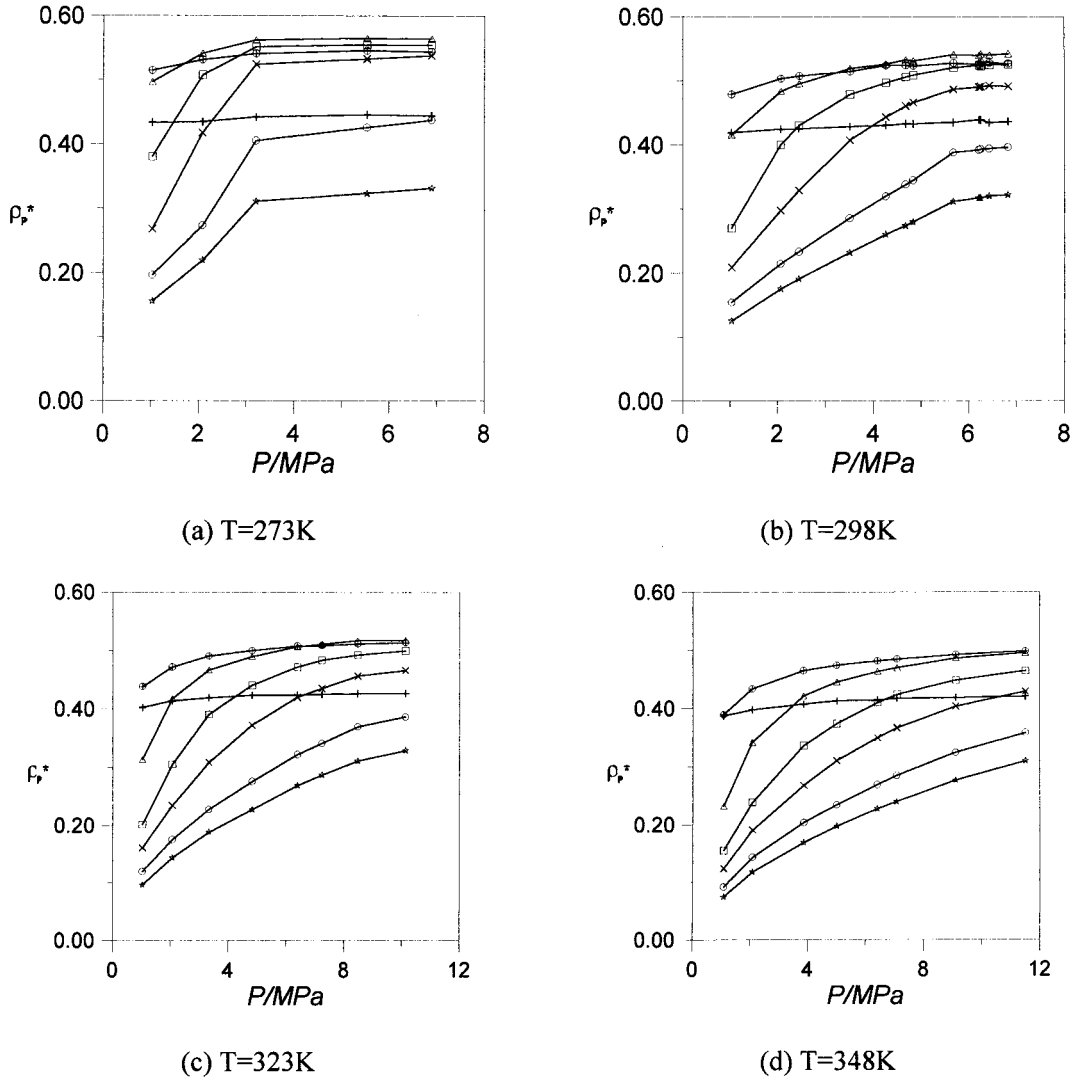

Figure 1. Adsorption isotherms at two subcritical temperatures and two supercritical temperatures: (+), $H^* = 2.0$; (⊕), $H^* = 3.0$; (△), $H^* = 4.0$; (□]), $H^* = 5.0$; (×), $H^* = 6.0$; (○), $H^* = 8.0$; (☆), $H^* = 10.0$.

"sphere-cylinder" micropore. Diestler et al.[20] and Somer and Davis[21] simulated the self-diffusion of LJ fluids constrained between two plane-parallel hard walls and the microscopic dynamics of fluids confined between smooth and structured walls, respectively. Klochko et al. investigated binary Ar−Kr systems in slit pores at 88 K[22] and ethane in graphite micropores.[23] Cracknell et al.[24] investigated the transport properties of methane in slit-shaped pores. They calculated the self-diffusion coefficients for pores of reduced width 2.5 and 3.0 nm at reduced temperature. It is still not clear about the diffusion behavior for slit pores of reduced width larger than 3.0 nm at temperatures near the critical point. Hammonds et al.[25] studied CO_2 monolayer physisorbed on the basal plane of graphite by computer simulation. However, their work was directed to determine the structure of the monolayer at relatively low temperatures between 100 and 130 K.

Table 1. Potential Parameters of Carbon Dioxide and Slit Carbon Wall[29]

CO_2		carbon wall	
σ_{ff}, nm	ϵ_{ff}/k, K	σ_{ss}, nm	ϵ_{ss}/k, K
0.372.	236.1	0.34	28.0

In this paper, we investigate the adsorption and diffusion behavior of CO_2 in slit carbon pores from subcritical temperatures to supercritical temperatures by using both the grand-canonical Monte Carlo (GCMC) and MD methods, and examine the effects of temperature, pressure, and slit width on the adsorption isotherms and diffusion coefficients in pores.

2. Potential Models

The fluid−fluid interaction is modeled by the cut and shifted LJ potential[7]

$$\phi_{ff} = \begin{cases} \phi_{LJ}(r) - \phi_{LJ}(r_c) & r < r_c \\ 0 & r \geq r_c \end{cases} \quad (1)$$

where r is the intermolecular distance, r_c is the cutoff

(20) Diestler, D. J.; Schoen, M.; Hertzner, A. W.; Cushman, J. H. *J Chem. Phys.* **1991**, *95*, 5432.
(21) Somers, S. A.; Davis, H. T. *J. Chem. Phys.* **1992**, *96*, 5389.
(22) Klochko, A. V.; Piotrovskaya, E. M.; Brodskaya, E. A. *Langmuir* **1996**, *12*, 1578.
(23) Klochko, A. V.; Brodskaya, E. A.; Piotrovskaya, E. M. *Langmuir* **1999**, *15*, 545.
(24) Cracknell, R. G.; Nicholson, D.; Gubbins, K. E. *J. Chem. Soc., Faraday Trans.* **1995**, *91*, 1377.
(25) Hammonds, K. D.; McDonald, I. R.; Tildesley, D. J. *Mol. Phys.* **1990**, *70*, 175.

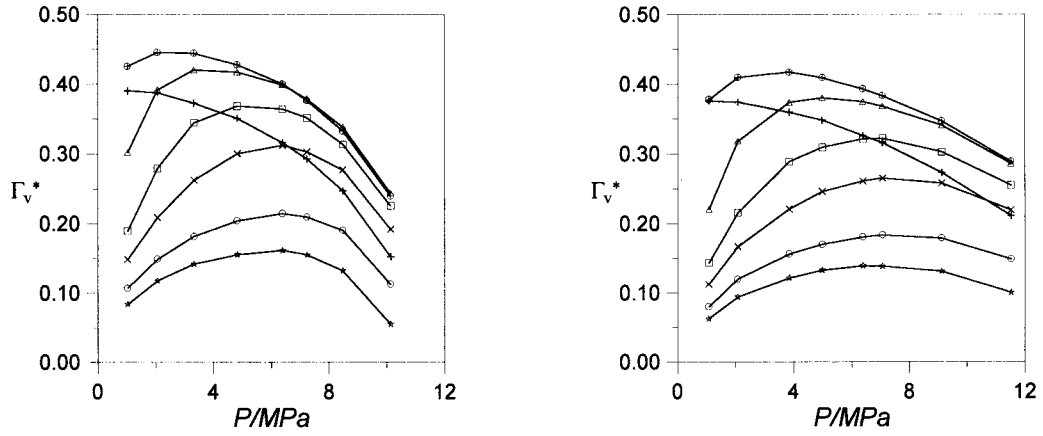

Figure 2. Excess adsorption isotherms at 323 and 348 K: (+), $H^* = 2.0$; (⊕), $H^* = 3.0$; (△), $H^* = 4.0$; (□), $H^* = 5.0$; (×), $H^* = 6.0$; (○), $H^* = 8.0$; (☆), $H^* = 10.0$.

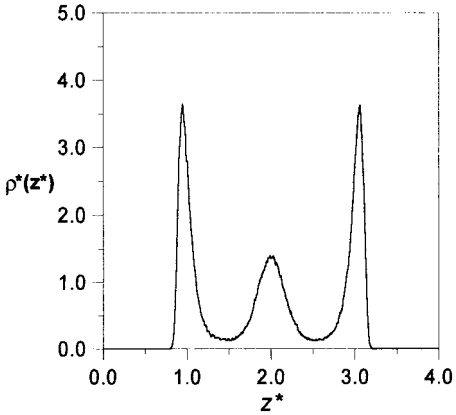

Figure 3. Local density profile of a slit pore of width $H^* = 4.0$ at 323 K and 7.24 MPa.

radius, $r_c = 2.5\sigma_{ff}$, ϕ_{LJ} is the full LJ potential

$$\phi_{LJ}(r) = 4\epsilon_{ff}\left[\left(\frac{\sigma_{ff}}{r}\right)^{12} - \left(\frac{\sigma_{ff}}{r}\right)^{6}\right] \quad (2)$$

where ϵ_{ff} and σ_{ff}, shown in Table 1, are the LJ energy and size parameters between two CO_2 molecules, respectively. It is noticeable that, although the LJ model is a simplified representation of CO_2, Zhou et al.[26−28] have used it to predict the self-diffusion coefficients of supercritical CO_2 with satisfaction.

The interaction between a solid wall and a fluid molecule is described by Steele's 10−4−3 solid−fluid potential[29]

$$\phi_{sf}(z) = 2\pi\rho_s\epsilon_{sf}\sigma_{sf}^2\Delta\left(\frac{2}{5}\left(\frac{\sigma_{sf}}{z}\right)^{10} - \left(\frac{\sigma_{sf}}{z}\right)^{4} - \left(\frac{\sigma_{sf}^4}{3\Delta(0.61\Delta + z)^3}\right)\right) \quad (3)$$

where ρ_s is the number density of solid carbon, $\rho_s = 114$ nm^{-3}, and the subscript s represents the solid wall, Δ is the distance between lattice planes, $\Delta = 0.335$ nm, z is the normal distance between a fluid molecule and one of the solid walls, ϵ_{sf} and σ_{sf} are the cross interaction parameters, which are obtained by the Lorentz−Berthelot combining rules. The interaction parameters of carbon walls are also shown in Table 1.

For a fixed slit width, the total potential energy of the adsorbate−adsorbent interaction ϕ_{sf} is the sum of the interaction with both carbon walls

$$\Phi_{sf} = \phi_{sf}(z) + \phi_{sf}(H - z) \quad (4)$$

where H is the slit width.

3. Molecular Simulation Methods

We first used GCMC simulation for the adsorption of CO_2 in slit pores. In our simulations, the periodic boundary conditions[8] were imposed only in parallel directions. The adsorbent surface area A was set to $180\sigma_{ff}^2$. In each simulation, 4×10^7 configurations were generated. The first 2×10^7 configurations were discarded to guarantee equilibration, whereas the second 2×10^7 configurations were used to average the desired thermodynamic properties. Simulation details can be referred to our previous work.[11]

Then, a constant-temperature MD by temperature scaling[7] was used to obtain the diffusion coefficients of CO_2 in pores. The equations of motion were solved by the fifth-order Gear predictor−corrector algorithm.[31] The reduced time step was 0.005. The overall density of a MD system was determined by the equilibration density of the GCMC simulation performed in advance. The total simulation length was 300 000 steps. The first 50 000 steps were used to equilibrate the system, while the second 250 000 steps were used to sample the diffusion properties of interest.

In our simulations, all variables were reduced with respect to CO_2 parameters. They are defined as follows.

$$\mu^* = \mu/\epsilon_{ff}, \quad z^* = z/\sigma_{ff}, \quad T^* = kT/\epsilon_{ff}$$

$$H^* = H/\sigma_{ff}, \quad \rho^* = \rho\sigma_{ff}^3, \quad A^* = A/\sigma_{ff}^2$$

where μ is the chemical potential, T is the temperature of the system, ρ is the number density of the fluid, A

(26) Zhou, J.; Lu, X.; Wang, Y.; Shi, J. *J. Chem. Ind. Eng. (China)* **1999**, *50*, 491.
(27) Zhou, J.; Lu, X.; Wang, Y.; Shi, J. *Chemi. J. Chin. Univ.* **2000**, *21*, 762.
(28) Zhou, J.; Lu, X.; Wang, Y.; Shi, J. *Fluid Phase Equilib.*, in press.

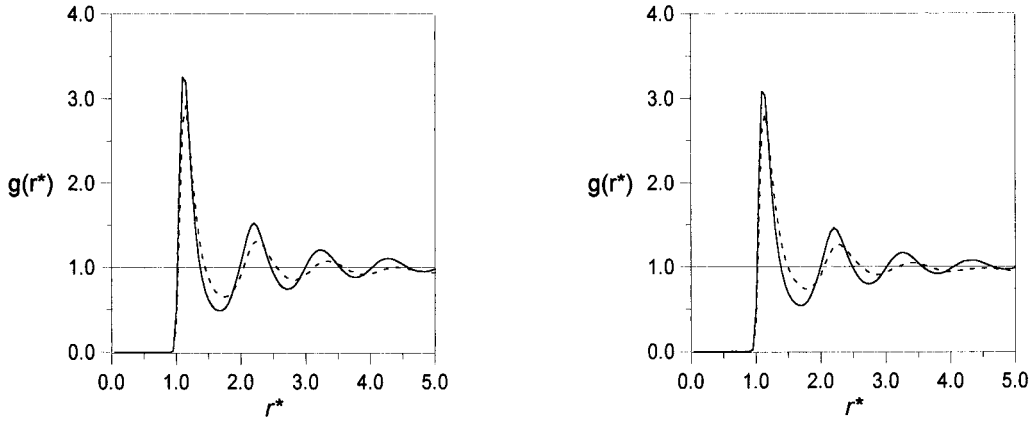

Figure 4. In-layer pair correlation functions for the slit pore of width $H^* = 4.0$ at 323 and 348 K and 7.24 MPa: (—), contact layer; (- - -), inner layer.

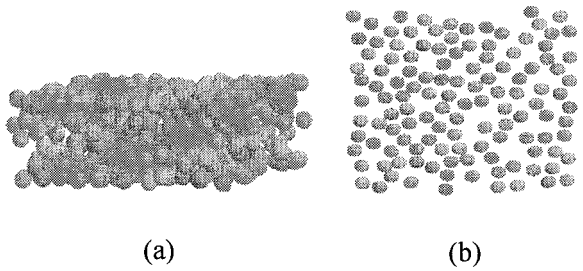

Figure 5. Snapshots for configurations of CO_2 molecules adsorbed in a slit pore of width $H^* = 6.0$ at 323 K and 7.24 MPa.

is the area of the slit wall, and k is the Boltzmann constant.

4. Results and Discussion

Both the GCMC and MD simulations were carried out for CO_2 at two subcritical temperatures, 273 K ($T_r = 0.90$) and 298 K ($T_r = 0.98$), and two supercritical temperatures, 323 K ($T_r = 1.06$) and 348 K ($T_r = 1.14$), for seven slit pores of $H^* = 2.0$, 3.0, 4.0, 5.0, 6.0, 8.0, and 10.0, corresponding from 0.74 to 3.72 nm. Accordingly, the adsorption isotherms, local density profiles, in-layer pair correlation functions and diffusion coefficients were calculated.

4.1. Adsorption Isotherms of CO_2. The adsorption isotherm is represented by the overall average reduced density ρ_p^*in a pore, which is given by

$$\rho_p^* = \frac{1}{H^*}\int_0^{H^*} \rho_p^*(z^*)\, dz^* \qquad (5)$$

where $\rho_p^*(z^*)$ is the local density distribution function, which can be solved in our simulations (see eq 6).

Figure 1a−d shows the simulated adsorption isotherms at 273, 298, 323, and 348 K. At each temperature, the adsorption isotherm increases with pressure up to a saturated value gradually, except for the pores of $H^* = 2.0$ and 3.0. The latter pores have stronger adsorption power at low pressures because of the deeper potential well, while the adsorption almost remains unchanged at higher pressures for the steric effect. For slit pores of $H = 4.0$, 5.0, and 6.0, the density reaches a larger value at relatively lower pressures. Lower pressures required for supercritical reaction processes lead to significant reduction in compression costs. Moreover, higher density of the pore fluid is favorable for dissolving the waxlike compounds and preventing the catalyst pore being clogged. In contrast, the density of the fluid inside the pores of $H^* = 8.0$ and 10.0 at 323 and 348 K increases insignificantly with pressure, because of the weaker interaction between the walls and the molecules in the center of the pores. For a constant pore width, the adsorption decreases with the increase of temperature, as is expected.

Figure 2a,b displays the excess adsorption isotherms expressed by the excess adsorption per unit of volume, Γ_v^*, for supercritical CO_2 at 323 and 348 K, where $\Gamma_v^* = \rho_p^* - \rho_b^*$, and $\rho_b^* = \rho_b \sigma_{ff}^3$ is the reduced bulk density. For each slit pore of width $H^* > 2.0$, Γ_v^* shows a maximum. This is in qualitative agreement with experimental measurements[31,32] and the simulations for methane and ethylene,[13] nitrogen, and hydrogen.[33] As the pore size increases, the maximum value declines and occurs at higher pressures, because the interactions between the fluid molecules and the walls become less significant. Naturally, the excess adsorption of each slit pore at 323 K is larger than that at 348 K.

4.2. Microstructure of CO_2 in Slit Carbon Pores. The microscopic structure of CO_2 confined in a slit pore is described by the local density profile $\rho_p^*(z^*)$, which is given by

$$\rho_p^*(z^*) = \langle N(z^*)\rangle/(A^*\cdot\Delta z^*) \qquad (6)$$

where $\langle N(z^*)\rangle$ is the ensemble average of the number of fluid molecules in a bin $A^*\cdot\Delta z^*$, and $\Delta z^* = 0.01$.

Figure 3 shows a local density profile of CO_2 molecules adsorbed in a slit pore of $H^* = 4.0$ at 323 K and 7.24 MPa. For the pore of $H^* = 4.0$, both the contact layer and inner layer are observed. Similar results are obtained at the other temperatures and pressures.

(29) Steele, W. A. *Surf Sci.* **1973**, *36*, 317.
(30) Gear, C. W. *Numerical Integration of Ordinary Differential Equations;* Prentice-Hall: Englewood Cliffs, NJ, 1971.
(31) Chen, J. H.; Wong, D. S. H.; Tan, C. S.; Subramanian, R.; Lira, C. T.; Orth, M. *Ind. Eng. Chem. Res.* **1997**, *36*, 2808.
(32) Malbrunot, P.; Vidal, D.; Vermesse, J.; Chahine, R.; Bose, T. K. *Langmuir* **1997**, *13*, 539.
(33) Darkrim, F.; Vermesse, J.; Malbrunot, P.; Levesque, D. *J. Chem. Phys.* **1999**, *110*, 4020.

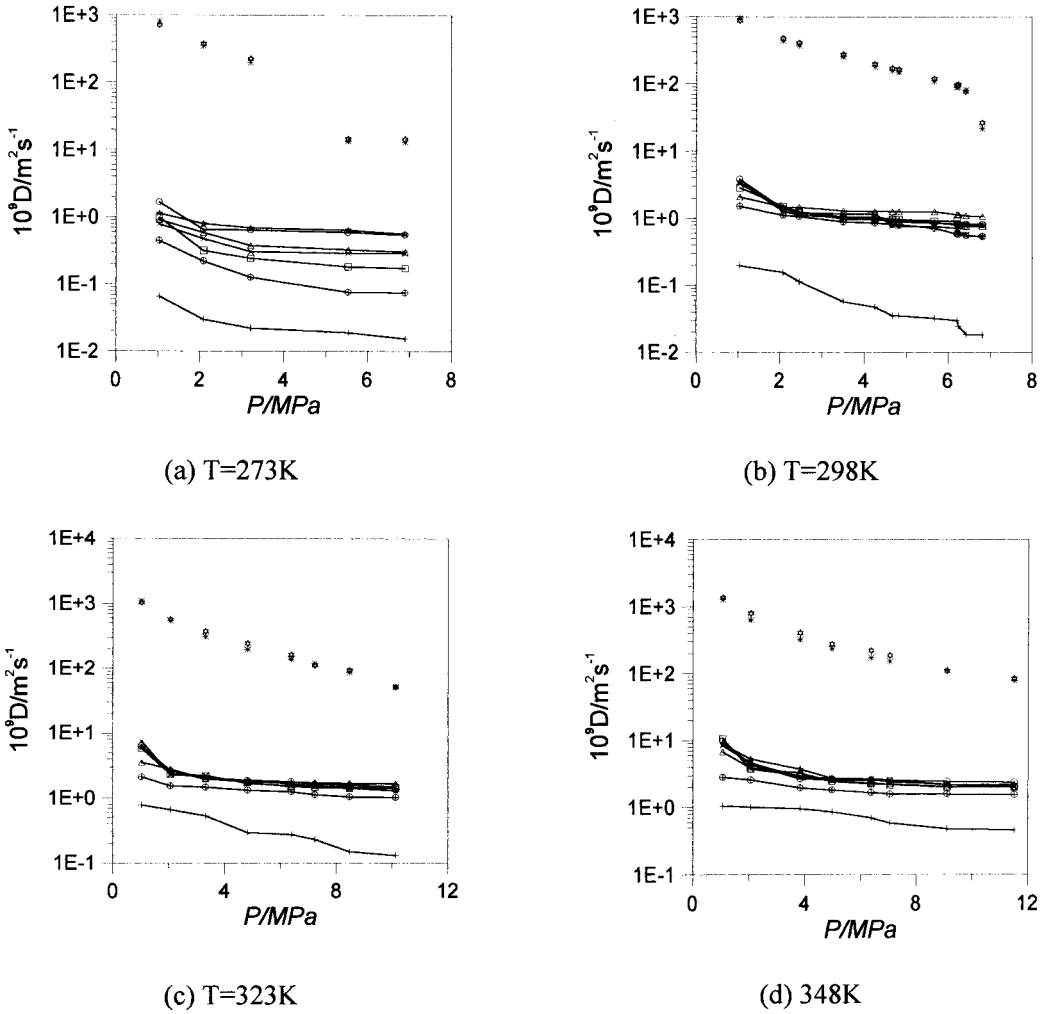

Figure 6. Parallel diffusion coefficients of CO_2 molecules confined in slit pores in supercritical and subcritical conditions: (+), $H^* = 2.0$; (⊕), $H^* = 3.0$; (△), $H^* = 4.0$; (□), $H^* = 5.0$; (×), $H^* = 6.0$; (○), $H^* = 8.0$; (☆), $H^* = 10.0$; (✡) simulation result of the bulk fluid[28]; (∗) experimental value of the bulk fluid.[34]

To further describe the microstructure of CO_2 confined in a slit pore, the in-layer pair correlation functions of the contact and inner layers were calculated. For illustration, some results are given in Figure 4 for the slit pore of $H^* = 4.0$ at 7.24 MPa, 323 and 348 K, respectively. It is found that both the contact and inner layers show a typical liquidlike structure. The contact layers present more ordered structure than the inner layers, which is due to the stronger interaction with the pore walls. Naturally, the contact layer at 323 K gives a more ordered structure than that at 348 K.

To characterize the microstructure more directly, Figure 5a shows a snapshot of CO_2 molecules confined in a slit pore of $H^* = 6.0$ at 323 K, while Figure 5b displays the picture of the contact layer. Obviously, the contact layer fluid exhibits the liquidlike structure.

4.3. Diffusion. Transport properties of fluid molecules can be calculated either from the Einstein relation or from the Green−Kubo approach.[7] In this work, both the diffusion coefficients parallel to the wall, $D_{||}$, and perpendicular to the wall, $D_\perp$, for the molecules in a pore are determined by the Einstein relation, i.e., from the long-time limiting slope of mean square displacements (MSD) versus time. In our MD simulations, they are given by $D_{||} = \langle \Delta x2(t) + \Delta y^2(t) \rangle / 4t$, and $D_\perp = \langle \Delta z^2(t) \rangle / 2t$, where brackets $\langle\ \rangle$ denote an ensemble average, t is the time, and Δx^2, Δy^2, and Δz^2 are the square displacements in each direction, respectively.

The values of $D_{||}$ and $D_\perp$ for subcritical and supercritical CO_2 confined in slit pores are shown in Figures 6a−d and 7a−d, respectively. As is seen in Figure 6, with the increase of pressure, $D_{||}$ decreases and reaches a limiting value at higher pressures, which is due to the increase of adsorption loading and the decrease of the free volume. The density of the fluid inside the pore plays an important role in determining the mobility of the fluid in a pore. In Figure 6, we also display the self-diffusion coefficients of CO_2 in the bulk phase at the same temperature and pressure by our previous simulations[28] and experiments of Etesse et al.[34] for comparison. The self-diffusion coefficients of the bulk fluid are several dozen times larger than $D_{||}$'s, because the bulk CO_2 is in the gas phase, while CO_2 in pores is liquidlike with much higher density. It is also found in Figure 6 that the magnitude of $D_{||}$ for CO_2 in pores is on the order of 10^{-9} $m^2 \cdot s^{-1}$, a typical liquidlike value. In addition, $D_{||}$ in the pore of $H^* = 2$ is much lower than that in the other pore sizes because of the deeper potential well and limited room for molecules to move around. This is consistent with the experiment.[18] It suggests that the diffusion rate within finely porous materials declines considerably when the molecule diameter becomes sig-

(34) Etesse, P.; Zega, A.; Kobayashi, R. *J. Chem. Phys.* **1992**, *97*, 2022.

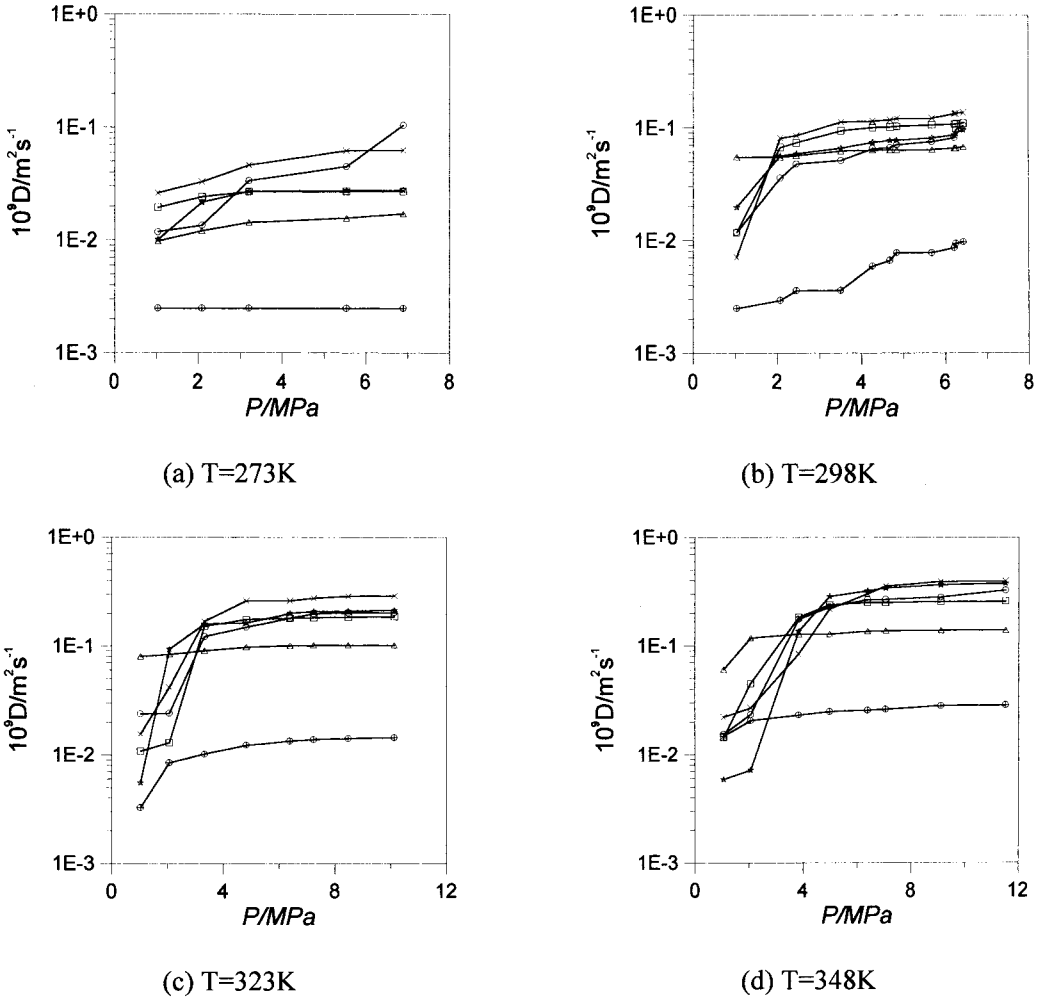

Figure 7. Perpendicular diffusion coefficients of CO_2 molecules confined in slit pores in supercritical and subcritical conditions: (⊕), $H^* = 3.0$; (△), $H^* = 4.0$; (□), $H^* = 5.0$; (×), $H^* = 6.0$; (○), $H^* = 8.0$; (☆), $H^* = 10.0$.

nificant with respect to the pore size; It is observed that, in general, the diffusivities increase slightly with slit width. For pores of $H^* \geq 4.0$, when the pressure is in the range of 2−10 MPa, $D_{||}$ is in the range $(1.3-2.8) \times 10^{-9}$ $m^2 \cdot s^{-1}$ at 323 K, while it is $(2.0-5.3) \times 10^{-9}$ $m^2 \cdot s^{-1}$ at 348 K.

Figure 7 gives the simulated perpendicular diffusion coefficients, which are important in diffusion-controlled heterogeneous catalytic reactions. The perpendicular diffusion coefficients for the pore of $H^* = 2.0$ are not presented here, because the molecules almost do not move in the normal direction. For the pore of $H = 3.0$, the values of D are much less than that in larger pores. This suggests that too small catalyst pores of $H^* = 2.0$ and 3.0 are dynamically not of practical use in supercritical reactions for CO_2. Consequently, by a combined consideration of adsorption and diffusion characteristics, catalysts of pore sizes $H^* = 4.0-6.0$ are suitable for the reactions in supercritical CO_2.

Self-diffusion coefficients have also been calculated for the bulk fluid at the same density as the average density of the pore fluid. A comparison among parallel diffusion coefficients, perpendicular diffusion coefficients of the pore fluid, and self-diffusion coefficients of the bulk fluid at the same density is shown in Figure 8a−f. For the fluid in pores of $H^* \geq 4.0$, the parallel diffusion is almost 10−20 times faster than the perpendicular diffusion. However, the differences between the values of parallel and perpendicular diffusion coefficients decrease gradually with the increase of the pore size. As is seen in Figure 8, the pore fluid molecules diffuse generally 1 order of magnitude slower in the parallel direction, compared with that in the bulk fluid at the same density. Obviously, the wall hinders the fluid diffusion inside the pore.

The temperature dependence of the diffusion coefficient in slit pores is plotted in Figures 9a−j. As is expected, the diffusion is enhanced with the temperature. For all of the pores investigated here, under higher pressures of industrial interests, both the diffusion coefficients parallel and normal to the walls at supercritical temperatures 323 K ($T_r = 1.06$) and 348 K ($T_r = 1.14$) are 5−15 times larger than those at subcritical temperatures 273 K ($T_r = 0.90$) and 298 K ($T_r = 0.98$). In this case, higher diffusion coefficients are favorable for speeding up the rates of supercritical catalytic reactions.

5. Conclusions

A combination of grand canonical Monte Carlo and molecular dynamics methods has been used to investigate adsorption and diffusion of carbon dioxide confined in seven slit carbon pores from 0.744 to 3.72 nm from subcritical to supercritical conditions. At supercritical temperatures, 323 and 348 K, each adsorption isotherm shows a maximum at a particular pressure. The maximum

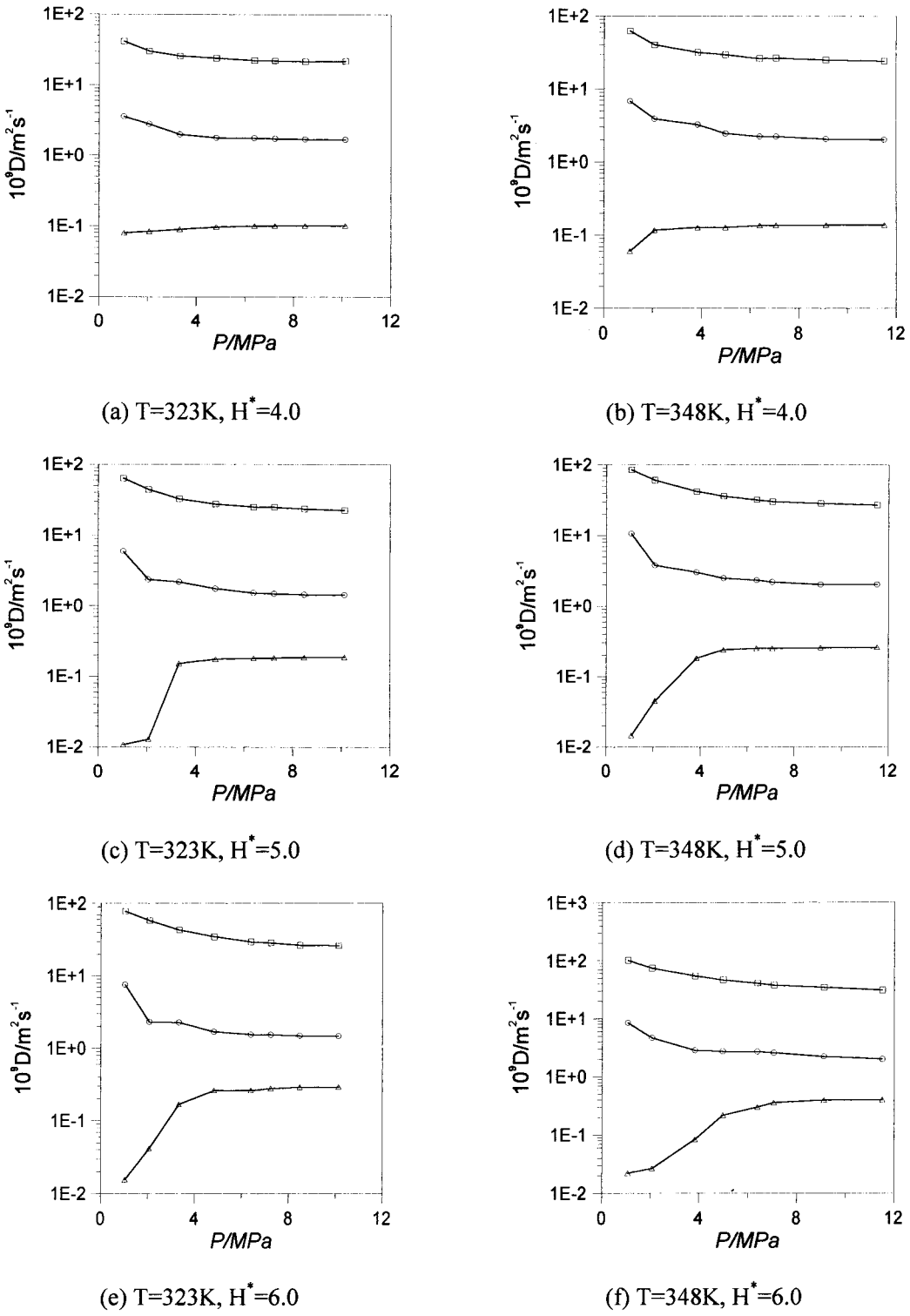

Figure 8. Diffusion coefficients of CO_2 molecules adsorbed in slit carbon pores. (○), parallel diffusion coefficients; (△), perpendicular diffusion coefficients; (□) diffusion coefficients of the bulk fluid at the same density as the mean density of the pore fluid.

adsorption declines and occurs at higher pressures with the increase of pore width, except for the narrow catalyst pores, e.g., $H^* = 2.0$ and 3.0 here. It indicates that the latter pores are dynamically unfavorable for supercritical reaction processes. In contrast, catalysts in the range $H^* = 4.0-6.0$ are suitable for supercritical reaction processes.

The diffusion coefficients of CO_2 molecules confined in a slit pore in supercritical conditions are strongly dependent on the density in the pore, which is obtained in the GCMC simulation in this work. The diffusion coefficients generally decrease with increasing density at a constant temperature. The magnitude of micropore fluid's $D_{||}$ is on the order of 10^{-9} $m^2 \cdot s^{-1}$, a typical liquidlike value. For pores of $H^* \geq 4.0$, the parallel diffusion is generally 10−20 times faster than the perpendicular diffusion. The difference between the parallel diffusion and the perpendicular diffusion decreases gradually with the increase of pore size. In general, the fluid molecules diffuse by 1 order of magnitude slower in the parallel direction than those in bulk phase at the same density. For the pores of $H^* \geq 4.0$, when the pressure is in the range 2−10 MPa, the

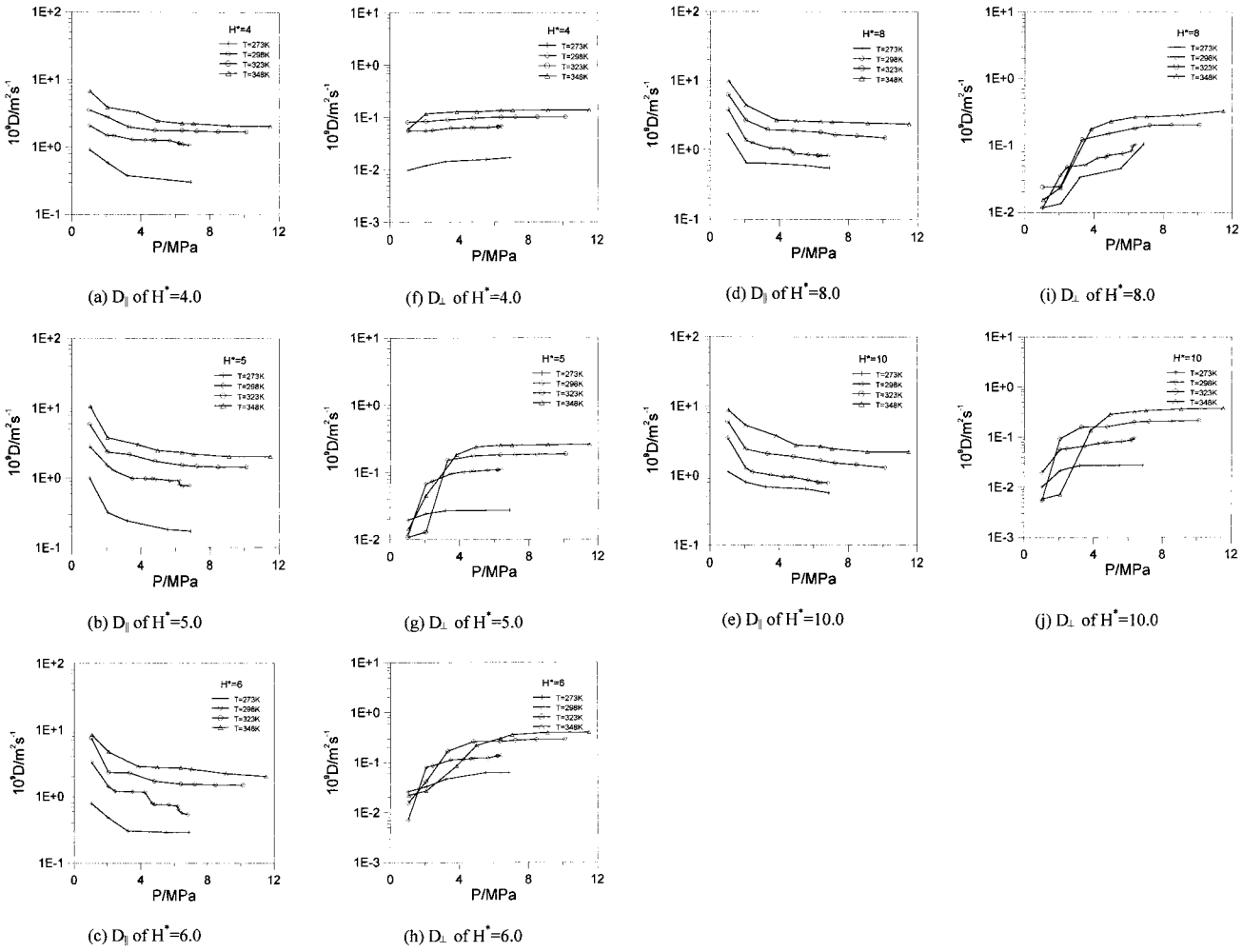

Figure 9. Effects of temperature on the parallel and perpendicular diffusion coefficients.

values of $D_{||}$ are in the range $(1.3-2.8) \times 10^{-9}$ $m^2 \cdot s^{-1}$ at 323 K, while they are $(2.0-5.3) \times 10^{-9}$ $m^2 \cdot s^{-1}$ at 348 K. Diffusion coefficients both parallel and normal to the walls at supercritical temperatures are 5−15 times larger than those at subcritical temperatures. Consequently, higher diffusion coefficients are favorable for speeding up the rates of supercritical catalytic reactions.

Acknowledgment. This work was supported by the National Natural Science Foundation of China under Grant No. 2977604 and National High Performance Computing Foundation of China under Grant No. 99118.

LA000216E